ISSN 1846-6168 (Print), ISSN 1848-5588 (Online)
ID: TG-20170816162744

Original scientific paper

THE INFLUENCE OF CHLORIDE ION CONCENTRATION ON THE CORROSION BEHAVIOR OF THE CuAlNi ALLOY

Ladislav VRSALOVIĆ, Ivana IVANIĆ, Diana ČUDINA, Lea LOKAS, Stjepan KOŽUH, Mirko GOJIĆ

Abstract: The influence of different chloride ion concentration (0.1 %, 0.5 %, 0.9 % and 1.5 % NaCl solution) on the electrochemical behaviour of the cast CuAlNi alloy was examined with electrochemical techniques (open circuit potential measurements, linear and potentiodynamic polarization measurements and electrochemical impedance spectroscopy (EIS)). After polarization measurements, electrode surfaces were examined with an optical microscope and the SEM/EDS analysis. Polarization measurements revealed that an increase in chloride ion concentration leads to an increase of the corrosion current density values and a decrease of the polarization resistance values, which indicated a higher corrosion attack on the alloy. The examination of alloy surfaces with an optical microscope and the SEM/EDS analysis has shown that there is no indication of pitting corrosion in the 0.1% NaCl solution, but pits were clearly visible on the samples which were examined in the higher chloride concentration solutions. The EDS analysis has shown the existence of copper oxide on the electrode surface and a presence of a small percentage of aluminium in the form of aluminium oxide.

Keywords: corrosion; CuAlNi alloy; electrochemical methods; SEM/EDS analysis; shape memory alloy

1 INTRODUCTION

Copper and copper alloys are widely used in the applications that require the mechanical strength associated with high thermal and electrical conductivity and good corrosion resistance [1]. The addition of aluminium to the Cu-based alloys increases its corrosion resistance due to the formation of the protective layer of alumina, which builds up quickly on the surface after the exposure to the corrosive environment. The presence of nickel is important in the passivation of Cu–Ni alloys because of its incorporation in the Cu(I) oxide which is formed on the corroded surface of the alloy and which reduces the number of cation vacancies that normally exist in the Cu(I) oxide [2-5].

CuAlNi alloys are potentially very attractive materials because of their shape memory effect. The shape memory effect has been observed in the Cu alloys with aluminium content close to 14 wt. percent and with varying nickel content [6]. The shape memory alloy (SMA) is an alloy that remembers its original shape when returning to the pre-deformed shape upon heating [7]. The shape memory effect is related to the solid state transformation of martensite to austenite and vice versa [8]. Nitinol (NiTi) is the most commonly used SMA due to its superior thermomechanical and thermoelectrical properties, combined with the high corrosion resistance and biocompatibility, but this alloy is very costly [9-11]. Cu-Al-Ni alloys have low production cost, better machinability, better work/cost ratio, they are easier to manufacture, and have a higher range of potential transformation temperatures [5, 11, 12].

Copper based shape memory alloys have been intensively studied from the viewpoints of metallography, fracture behaviour, mechanical properties and activation energy of the precipitate grow process, but relatively little attention has been devoted to their electrochemical behaviour [6-8, 10, 12-15]. As the practical application of Cu-SMA is constantly increasing, these alloys are exposed to different corrosion media for a longer period of time and that could lead to the appearance of corrosion damage on their surface, jeopardise their structural integrity and cause immense consequences if the corrosion processes are not observed in time. Therefore it is important to evaluate the corrosion behaviour of Cu-based SMAs in different environments, and also to improve their corrosion resistance before their industrial applications.

2 RESULTS AND DISCUSSION

Fig. 1 presented the results of the open circuit potential (E_{OCP}) measurements for the CuAlNi alloy in different chloride solutions.

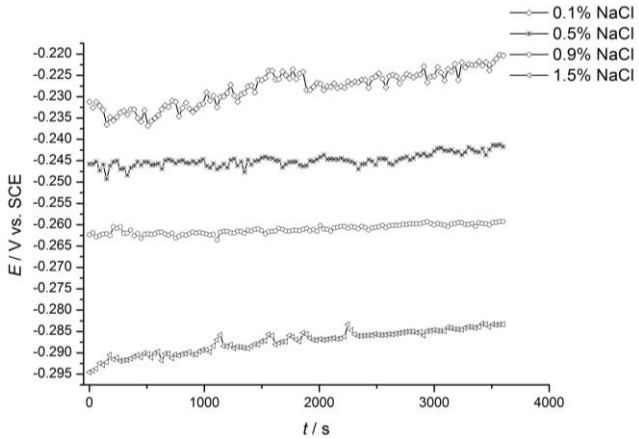

Figure 1 Open circuit potential vs. time curves for the CuAlNi alloy in chloride solutions

The open circuit potential is the potential of the working electrode relative to the reference electrode when no potential or current is being applied to the cell. The way in which a metal changes its potential upon immersion in

the solutions indicates the nature of the reaction which is taking place at its surface. Whilst a shift in potential towards more positive values denotes film formation and thickening, a shift in the negative direction signifies film destruction and the exposure of more of the bare metal to the aggressive solution [16].

From the Fig. 1 small changes in the potential of the CuAlNi alloy in a 60 minute period of time can be seen. The open circuit potentials of the CuAlNi electrodes have a tendency to shift towards the more negative values with increasing sodium chloride concentrations, so the highest difference between the E_{OCP} values for the CuAlNi alloy in the 0.1% NaCl solution and for the 1.5% NaCl solution was around 70 mV.

The electrochemical impedance spectra were taken after the E_{OCP} measurement and the results were shown in Fig.2 in the Nyquist and Bode complex plane.

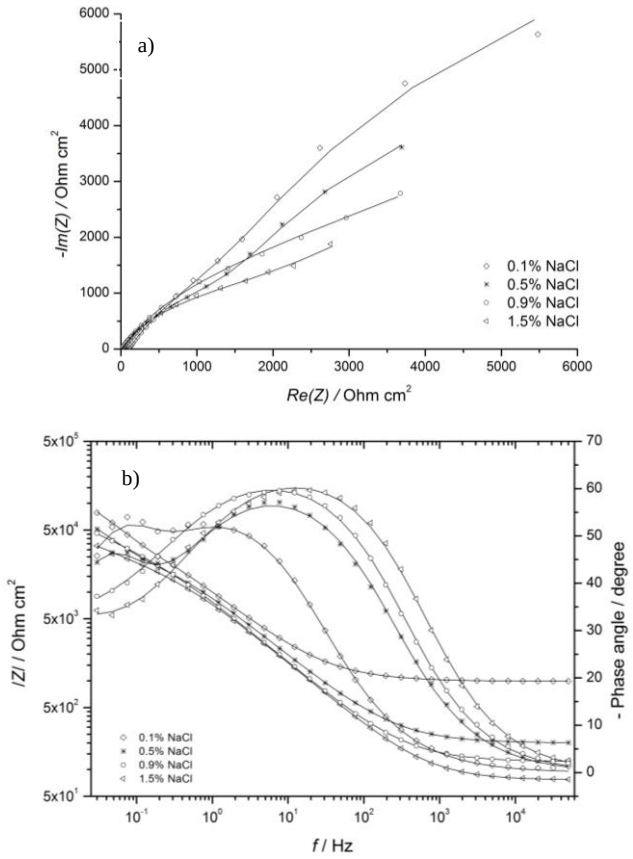

Figure 2 Nyquist a) and Bode b) plot of impedance spectra for the CuAlNi alloy in the 0.1% (-), 0.5% (-), 0.9% (-) i 1.5% (-) NaCl solution

The Nyquist plot, which represents the ratio of the imaginary (Z_{imag}) and real (Z_{real}) components of the impedance of the examined samples, shows fragments of a large incomplete semicircle. This is a typical impedance response for tin surface films. The observed time constants are partially overlapping and in such a graphic representation it is difficult to gain a clear insight into the results. From the Nyquist plot it is clearly visible that an increase in chloride concentration leads to a significant decrease of the diameter of the semicircle which indicates a lower corrosion resistance.

A more convenient method, which better shows the frequency dependence of the impedance data (and a clearer distinction between the individual time constants) is the so-called Bode diagram, i.e. the plots of the logarithm of impedance, Z, and the phase angle, respectively, *vs.* the logarithm of frequency, f. In this diagram (Fig. 2b), it is possible to observe three characteristic regions:

- In the high frequency region (f > 1 kHz), the log $|Z|$ values are low, tending towards the constant values, while the phase angle values fall rapidly towards 0°. This is a classic resistive response, corresponding to the electrolyte resistance.
- In the medium frequency region (f < 10 kHz), the linear log $|Z|$ *vs.* the log f relationship with a slope close to −1 and a phase angle of ≈ −70° mirror the capacitive behaviour of the system.
- At the lowest frequencies (f < 1 kHz), the phase angle of ≈ −20° and the slope of the log $|Z|$ vs. the log f close to −0.5 point towards the presence of a slow diffusion process.

The proposed equivalent circuit for the modelling of the impedance data is shown in Fig. 3. It consists of electrolyte resistance (R_{el}) connected with two time constants. The model is based on the circuits mostly used in literature for the simulation of the kinetics of the copper and copper alloy corrosion process and the protective properties of the surface corrosion product layer [3, 17-20].

The first time constant, observed in the high frequency region, is the result of the fast charge transfer process in the alloy dissolution reaction. In this case, R_1 represents the charge transfer resistance, and Q_1 represents the constant phase element and replaces the capacitance of the electrochemical double layer.

To account for the surface layer and the diffusion process in the low frequency range, additional equivalent circuit parameters were introduced, such as R_2 for the surface layer resistance, Q_2 for the constant phase element of the surface layer (Q_2 replaces the capacitance of the surface layer) and Warburg impedance, W, for the diffusion process.

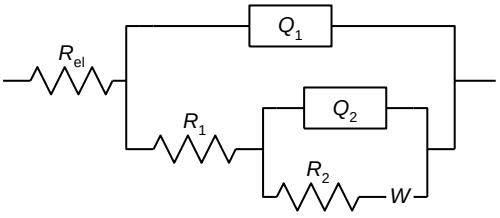

Figure 3 Proposed equivalent circuit for the modelling of the impedance data

The calculated equivalent circuit parameters for the CuAlNi alloy in a different chloride solution are presented in Tab. 1.

Table 1 Impedance parameters for the CuAlNi electrode in a different concentration of the NaCl solution

NaCl (%)	R_{el} (Ω)	$Q_1\times10^3$ ($F\times s^{n-1}$)	n_1	R_1 (Ω)	$Q_2\times10^3$ ($F\times s^{n-1}$)	n_2	R_2 (Ω)	W ($\Omega^{-1}s^{-1/2}$)
0.1	197.5	137.20	0.69	15238	101.30	1	32869	24.73
0.5	39.74	140.10	0.71	7293	301.30	0.99	13825	1491
0.9	24.54	153.50	0.73	6368	181.30	0.39	6113	7783
1.5	15.10	151.30	0.74	4653	431.60	0.50	1532	10339

After the impedance measurements, the linear polarization measurements were performed in the potential region of ±20 mV around E_{OCP}, and the results are shown in Fig. 4.

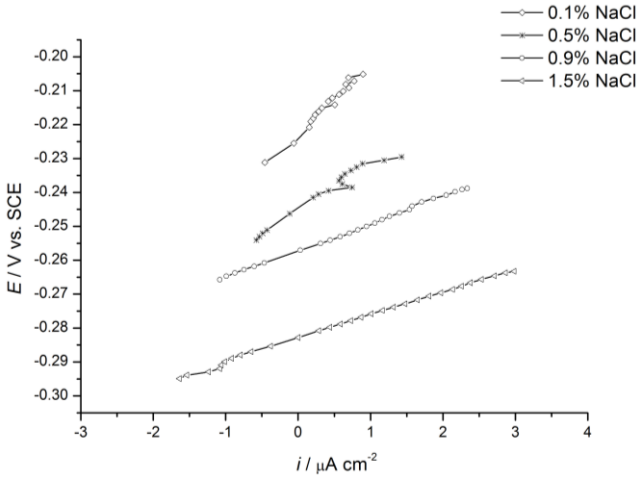

Figure 4 Linear polarization curves for the CuAlNi alloy in NaCl solutions

Polarization resistance (R_p) represents the resistance of metal to corrosion, and is defined by the slope of the polarization curve near the corrosion potential, by the Eq. (1):

$$R_p = \frac{\Delta E}{\Delta i}. \quad (1)$$

The values of corrosion resistance for the CuAlNi samples were shown in Tab. 2.

From Fig. 4 it can be seen that an increase in chloride concentration leads to a decrease of the slopes of the polarization curves, resulting in the lower values of R_p, which includes a lower resistance of the CuAlNi alloy to corrosion.

After the linear polarization measurements, potentiodynamic measurements were carried out in a wide range of potentials starting at −0.250 V from an open circuit potential and finishing at 1.100 V (Fig. 5).

The potentiodynamic polarization curve is composed of two branches: cathodic branch, which is the result of an occurring cathodic reaction and the anode part, which is the result of an occurring anodic reaction, in this case the alloy dissolution. The cathodic parts of polarization curves should reflect the hydrogen evolution reaction due to the deaeration of the solution with nitrogen, 20 minutes before the immersion of the electrode in electrolyte, as well as due to the slow deaeration during the examination.

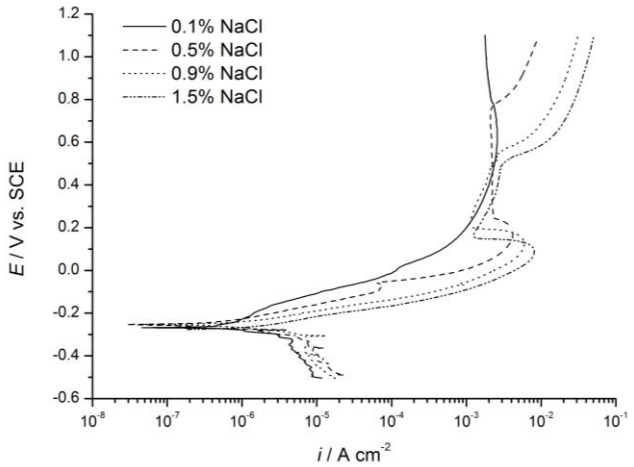

Figure 5 Potentiodynamic polarization curves for the CuAlNi alloy in NaCl solutions

Changes in the cathodic part of the polarization curves for the CuAlNi alloy in the NaCl solutions probably indicate the existence of a small concentration of oxygen in the solution, and therefore both cathodic reactions are possible: the oxygen reduction and hydrogen evolution reaction. The anodic parts of the curve describe the corrosion of the CuAlNi alloy. The anodic part of the polarization curve for the CuAlNi alloy in the 0.1% NaCl solution differs from the anodic parts of the polarization curves obtained by the CuAlNi alloy examinations in the higher concentrations of the NaCl solutions. This is probably due to the low concentration of chloride ions, which is why the anodic current density is significantly lower, indicating a weaker dissolution of the CuAlNi alloy. The anodic part of the polarization curves for the CuAlNi alloy in the 0.5, 0.9 and 1.5% NaCl solutions have three distinctive visible areas: the active dissolution region (apparent Tafel region), the active-passive transition region, and the third region in which the current density rises again with the positive potential changes due to the formation of Cu(II) species [21-23]. It is also clear that the values of the anode currents increase with the increase of the chloride ion concentration. The largest width of the pseudo-passive area was observed for the examinations of the CuAlNi alloys in the 0.5% NaCl solution, and the lowest width of the pseudo-passive area was noticed in the 1.5% NaCl solution. Moreover, after the dissolution of the corrosion products from the surface, the anodic current density increases in the following order: 0.5 % < 0.9 % < 1.5 % (area III in the anodic polarization curve).

The corrosion parameters obtained from the polarization measurements were shown in Tab. 2.

Table 2 Corrosion parameters obtained from the polarization measurements

NaCl (%)	R_p ($k\Omega\ cm^2$)	i_{corr} ($\mu A\ cm^{-2}$)	E_{corr} (V)
0.1	39.318	0.317	-0.220
0.5	29.000	0.551	-0.242
0.9	14.756	1.211	-0.259
1.5	12.886	2.041	-0.283

The data from Tab. 2 shows that an increased concentration of chloride ions leads to an increase in the corrosion current densities and a decrease in polarization resistance which indicates a higher corrosion of the CuAlNi alloy. It is also worthwhile mentioning that the recorded corrosion potential also decreased with an increase in chloride concentration.

After the polarization measurements, the corroded CuAlNi alloy surfaces were examined with an optical microscope with the magnification of 200 times. The results of the examinations were shown in Fig. 6 for the CuAlNi measurements in the 0.1, 0.9 and 1.5% NaCl solution.

It is interesting to note that at the lowest concentration of the NaCl solution, the presence of the pitting corrosion on the surface of the electrode was not observed, while in the examinations at the 0.9% and 1.5% NaCl solution, the pits were clearly visible on the surface of the CuAlNi electrodes. After the potentiodynamic polarization measurement in the 0.9% NaCl solution, a large number of smaller pits (Fig. 6b) were observed on the CuAlNi alloy surface, while in the 1.5% solution, a lower number of pits with a much larger diameter were noticed (Fig. 6c).

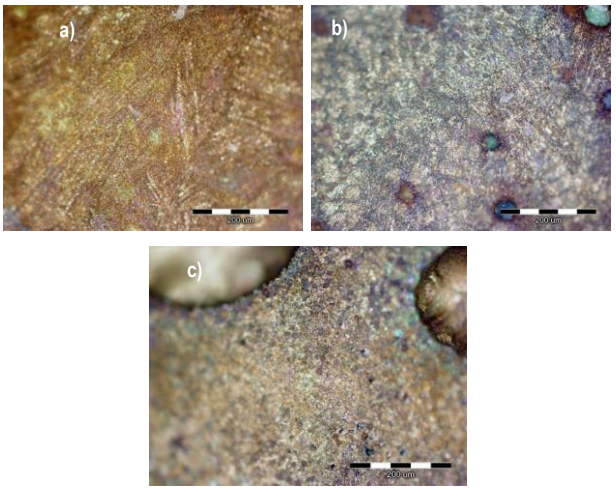

Figure 6 Optical micrographs of the CuAlNi alloy surfaces after the potentiodynamic polarization in the 0.1% a), 0.9% b) and 1.5% NaCl solution c)

The morphology of the alloy surfaces was examined by the SEM and EDS analysis and the results were presented in Fig. 7 for the CuAlNi alloy after the polarization measurements in the 0.9% NaCl solution.

The SEM/EDS surface analysis confirmed the observations obtained by examining the surface with an optical microscope. Pitting corrosion was not detected on the CuAlNi alloy surfaces which were examined in the 0.1% NaCl solution, while polarization examination in the higher chloride concentration leads to a pitting corrosion on the CuAlNi alloy.

In Fig.7 small pits are clearly visible, as is the rough surface of the corrosion products around them. The EDS analysis of the surface outside the pits revealed an elementary composition of the corrosion products on the surface of the CuAlNi electrodes. On the corrosion surface layer, the dominant elements were Cu and Cl, with small amounts of O, Al, and Ni, which confirms the observations of Benedetti and associates [21] on the formation of the aluminium oxide surface layer during the corrosion process of the Cu-Al alloys.

The analysis of the surface inside the pit showed a significantly higher percentage of chlorine relative to the surface around the pit, indicating that the corrosion inside the pits occurred by the formation of a soluble corrosive products of the copper chloride.

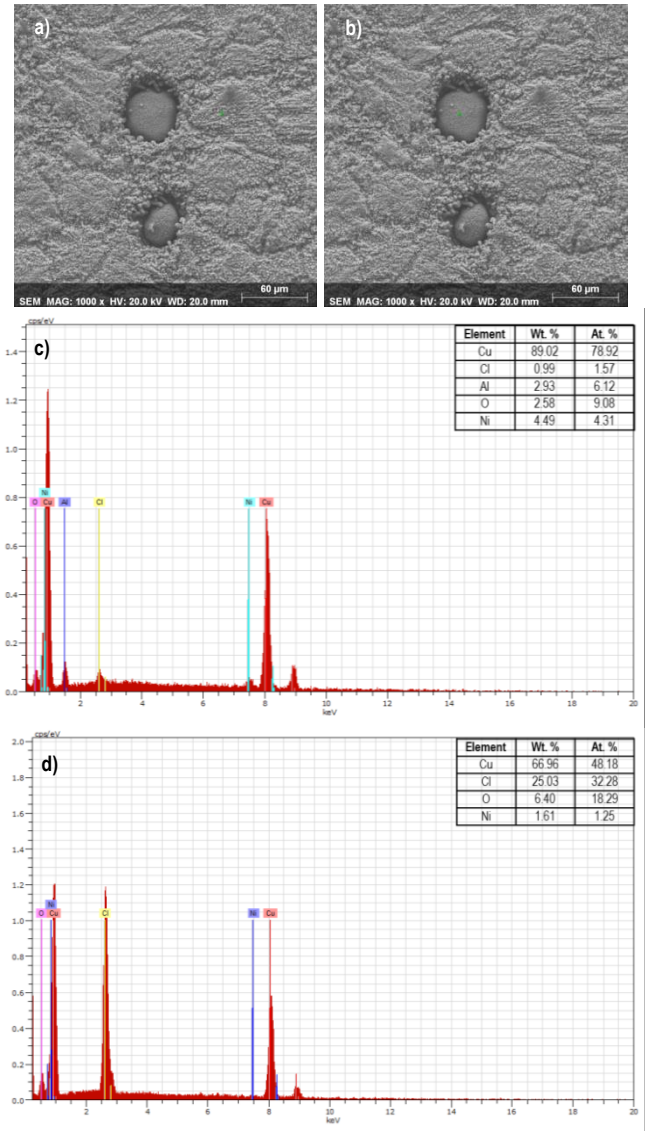

Figure 7 SEM micrograph with a marked position for the EDS analysis outside the pit a), inside the pit b), EDS results outside the pit c) and inside the pit d) for the CuAlNi alloy after the polarization measurements in the 0.9% NaCl solution

3 CONCLUSION

The open circuit potential for the CuAlNi alloy shifts to a negative direction with an increase in the concentration of chloride ions in the solution.

The results of the electrochemical impedance spectroscopy examinations showed that the overall

impedance of the system was reduced by increasing the chloride ion concentration.

A higher concentration of chloride ions leads to a lowering polarization resistance values and an increase in the corrosion current values, which indicates a more intense corrosion process.

The optical microscopy analysis of the electrode surfaces has shown the appearance of the pitting corrosion on the CuAlNi alloy after the polarization examinations in the 0.5%, 0.9% and 1.5% NaCl solutions.

The morphology examination of the alloy surfaces with SEM has confirmed the observations obtained by examining the electrode surfaces with an optical microscope. The largest number of pits is visible on the CuAlNi alloy surface after the corrosion examination in a 0.9% NaCl solution, while the largest diameter pits were recorded after the polarization in the 1.5% NaCl solution

The EDS surface analysis has shown the dominant percentage of copper and oxygen on the CuAlNi surface indicating the existence of copper oxide on the surface. The presence of a small percentage of aluminium indicates its distribution in the form of aluminium oxide on the surface layer.

Acknowledgements

This work has been fully supported by the Croatian Science Foundation under the project IP-2014-09-3405.

Note: Part of this research was presented at the International Conference MATRIB 2017 (29 June - 2 July 2017, Vela Luka, Croatia).

4 REFERENCES

[1] Liberto, R. C. N.; Magnabosco, R.; Alonso-Falleiros, N. Selective Corrosion in Sodium Chloride Aqueous Solution of Cupronickel Alloys with Aluminum and Iron Additions. // Corrosion. 63, (2007), pp. 211-219.

[2] Schussler, A.; Exner, H. E. The corrosion of nickel-aluminium bronzes in seawater—II. The corrosion mechanism in the presence of sulphide pollution. // Corrosion Science. 34, 11(1993), pp. 1803-1811.

[3] Badawy, W. A.; El-Sherif, R. M.; Shehata H. Electrochemical stability of Cu-10Al-5Ni alloy in chloride-sulphate electrolytes. // Electrochimica Acta. 54, 19(2009), pp. 4501-4505.

[4] Nady, H.; Helal N. H.; Rabiee, M. M.; Badawy, W. A. The role of Ni content on the stability of Cu-Al-Ni ternary alloy in neutral chloride solutions. // Materials Chemistry and Physics. 134, 2-3(2012), pp. 945-950.

[5] Gojić, M.; Vrsalović, L.; Kožuh, S.; Kneissl, A.; Anžel, I.; Gudić, S.; Kosec, B.; Kliškić, M. Electrochemical and microstructural study of Cu-Al-Ni shape memory alloy. // Journal of Alloys and Compounds. 509, 41(2011), pp. 9782-9790.

[6] Husain, S. W.; Clapp, P. C. The effect of aging on the fracture behavior of Cu-Al-Ni β phase alloys. // Metallurgical transactions A. 19A, (1988), pp. 1761-1766.

[7] Sathish, S.; Mallik, U. S.; Raju, T. N. Microstructure and shape memory effect of Cu-Zn_Ni shape memory alloys. // Journal of Minerals and Materials Characterization and Engineering. 2, (2014), pp. 71-77.

[8] Raju, T. N.; Sampath, V. Influence of aluminium and iron contents on the transformation temperatures of Cu-Al-Fe shape memory alloys. // Transactions of the Indian Institute of Metals. 64, 1-2(2011), pp. 165-168.

[9] Cai, W.; Meng, X. L.; Zhao, L. C. Recent development of TiNi-based shape memory alloys. // Current Opinion in Solid State and Material Science. 9, 9(2005), pp. 296-302.

[10] Kneissl, A. C.; Unterweger, E.; Bruncko, M.; Lojen, G.; Mehrabi, K.; Scherngell, H. Microstructure and properties of NiTi and CuAlNi Shape memory alloys. // Metallurgical & Materials Engineering. 14, 2(2008), pp. 89-100.

[11] Ivanić, I.; Gojić, M.; Kožuh, S. Shape Memory Alloys (Part II): Classification, Production and Application. // Kemija u industriji. 63, 9-10(2014), pp. 331-344.

[12] Čolić, M.; Rudolf, R.; Stamenković, D.; Anžel, I.; Vučević, D.; Jenko, M.; Lazić, V.; Lojen, G. Relationship between microstructure, cytotoxicity and corrosion properties of Cu-Al-Ni shape memory alloy. // Acta Biomaterialia. 6, 1(2010), pp. 308-317.

[13] Živković, D.; Holjevac Grgurić, T.; Gojić, M.; Čubela, D.; Stanojević Šimšić, Z.; Kostov, A.; Kožuh, S. Calcualtion of thermodynamic properties of Cu-Al-(Ag,Au) shape memory alloy systems. // Transactions of the Indian Institute of Metals. 67, 2(2014), pp. 285-289.

[14] Kumar Jain, A.; Hussain, S.; Kumar, P.; Pandey, A.; Dasgupta, R. Effect of varying Al/Mn ratio on phase transformation in Cu-Al-Mn shape memory alloys. // Transactions of the Indian Institute of Metals. 69, 6(2016), pp. 1289-1295.

[15] Ivanić, I.; Kožuh, S.; Kosel, F.; Kosec, B.; Anžel, I; Bizjak, M.; Gojić M. The influence of heat treatment on fracture surface morphology of the CuAlNi shape memory alloy. // Engineering Failure Analysis. 77, (2017), pp. 85-92.

[16] El Desouky, H.; Aboeldahab, H. A.: Effect of Chloride Concentration on the Corrosion Rate of Maraging Steel. // Open Journal of Physical Chemistry. 4, (2014), pp. 147-165.

[17] Cicileo, G.; Rosales, B.; Varela, F.; Vilche, J.: Comparative study of organic inhibitors of copper corrosion. // Corrosion Science. 41, 7(1999), pp. 1359-1375.

[18] Zhang, D.; Gao, L.; Zhou, G. Inhibition of copper corrosion by bis-(1-benzotriazolymethylene)-(2,5-thiadiazoly)-disulfide in chloride media. // Applied Surface Science. 225, 1-4(2004), pp. 287-293.

[19] Srivastava, A.; Balasubramaniam, R. Electrochemical Impedance Spectroscopy Study of Surface Films Formed on Copper in Aqueous Environments. // Materials and Corrosion. 56, 9(2005), pp. 611-618.

[20]Badawy, W. A.; Ismail, K. M.; Fathi, A. M. Effect of Ni content on the corrosion behavior of Cu–Ni alloys in neutral chloride solutions. // Electrochimica Acta. 50, 18(2005), pp. 3603-3608.
[21]Benedetti, A. V.; Sumodjo, P. T. A.; Nobe, K.; Cabot, P. L.; Proud, W. G. Electrochemical studies of copper, coper-aluminium and copper-aluminium-silver alloys: Impedance results in 0.5 M NaCl. // Electrochimica Acta. 40, 6(1995), pp. 2657-2668.
[22]Rosatto, S. S.; Cabot, P. L.; Sumodjo, P. T. A.; Benedetti, A. V. Electrochemical studies of coper-aluminium-silver alloys in 0.5 M H_2SO_4. // Electrochimica Acta. 46, 7(2001), pp. 1043-1051.
[23] Kear, G; Barker, B. D.; Walsh, F. C. Electrochemical corrosion of unalloyed copper in chloride media – a critical review. // Corrosion Science. 46, 1(2004), pp. 109-135.

Authors' contacts:

Dr. Sc. Ladislav VRSALOVIĆ, Associate Professor
University of Split, Faculty of Chemistry and Technology
Ruđera Boškovića 35, 21000 Split, Croatia
Tel. 021 329 444, Fax. 021 329 461, e-mail: ladislav@ktf-split.hr

Dr. Sc. Ivana IVANIĆ,
University of Zagreb, Faculty of Metallurgy,
Aleja narodnih heroja 3, 44103 Sisak, Croatia

Diana ČUDINA, M. Ch. E.
University of Split, Faculty of Chemistry and Technology
Ruđera Boškovića 35, 21000 Split, Croatia
Tel. 021 329 444, Fax. 021 329 461,
e-mail: diana.cudina@gmail.com

Lea LOKAS, M. Ch. E., Senior Associate
Development-Innovation Center AluTech,
Velimira Škorpika 6, 22000 Šibenik, Croatia

Dr. Sc. Stjepan KOŽUH, Associate Professor
University of Zagreb, Faculty of Metallurgy,
Aleja narodnih heroja 3, 44103 Sisak, Croatia

Dr. Sc. Mirko GOJIĆ, Full Professor
University of Zagreb, Faculty of Metallurgy,
Aleja narodnih heroja 3, 44103 Sisak, Croatia